Bioorganic & Medicinal Chemistry 19 (2011) 4608–4615

Contents lists available at ScienceDirect

Bioorganic & Medicinal Chemistry

journal homepage: www.elsevier.com/locate/bmc

Design, syntheses, and kinetic evaluation of 3-(phenylamino)oxazolidine-2,4-diones as potent cytochrome bc_1 complex inhibitors

Fu Wang [a,1], Hui Li [a,1], Le Wang [b], Wen-Chao Yang [a], Jia-Wei Wu [b,*], Guang-Fu Yang [a,*]

[a] Key Laboratory of Pesticide & Chemical Biology, Ministry of Education, College of Chemistry, Central China Normal University, Wuhan 430079, PR China
[b] MOE Key Laboratory of Bioinformatics, Department of Biological Sciences and Biotechnology, Tsinghua University, Beijing 100084, PR China

ARTICLE INFO

Article history:
Received 4 May 2011
Revised 2 June 2011
Accepted 2 June 2011
Available online 12 June 2011

Keywords:
Oxazolidinedione
Cytochrome bc_1 complex
Famoxadone

ABSTRACT

The cytochrome bc_1 complex (EC 1.10.2.2, bc_1) is one of the most promising targets for new drugs and agricultural fungicides. Among the existing bc_1 complex inhibitors specifically binding to the Q_o site, oxazolidinedione derivatives have attracted great attention. With the aim to understand the substituent effects of oxazolidinedione derivatives on the inhibition activity against the bc_1 complex, a series of new oxazolidinedione derivatives were designed, synthesized, and biologically evaluated. The further inhibitory kinetics studies against porcine succinate–cytochrome *c* reductase (SCR) revealed that the representative compound **8d** and famoxadone are both non-competitive inhibitors with respect to the substrate cytochrome *c*, but competitive inhibitors with respect to substrate decylubiquinol (DBH_2). In addition, compound **8d** and famoxadone showed, respectively, 35-fold and 15-fold greater inhibitory activity against the porcine SCR than the porcine bc_1 complex, indicating that these two inhibitors not only inhibited the activity of the bc_1 complex, but possibly affect the interaction between the complex II and the bc_1 complex. To our knowledge, this is the first report that famoxadone and its analogs have effects on the interaction between the complex II and the bc_1 complex.

1. Introduction

The cytochrome bc_1 complex (EC 1.10.2.2, bc_1) is an essential component of the cellular respiratory chain and the photosynthetic apparatus in photosynthetic bacteria. The function of the bc_1 complex is to catalyze the electron transfer from quinol to a soluble cytochrome *c* (cyt *c*) and couple this electron transfer to the translocation of protons across the membrane.[1–4] The bc_1 complex has a diheme cytochrome *b*, an iron–sulfur protein (ISP) with a Rieske-type Fe_2S_2 cluster, and cytochrome c_1 that undergo reduction and oxidation during the turnover of the enzyme. Due to its crucial role in the life cycle, inhibition of the bc_1 complex has become an important area for the discovery of fungicides useful in controlling crop diseases. So far, two separate catalytic sites of the bc_1 complex have been identified and have been confirmed by X-ray crystallographic studies: the quinol oxidation site (Q_o site) and the quinone reduction site (Q_i site). A number of inhibitors specifically binding to the Q_o site of the bc_1 complex, termed Q_oI fungicides, have been introduced into the agricultural fungicide market, including methoxyacrylate, oxazolidinedione and imidazolinone derivatives.[5]

Based on specific binding interactions and conformational changes observed in both cyt *b* and the ISP domain of the bc_1 complex, Q_o inhibitors can be further divided into two subgroups.[4] Subgroup I includes azoxystrobin (AZ) and any methoxyacrylate-type inhibitors, while subgroup II contains stigmatellin, famoxadone, and UHDBT. The ISP domain is still mobile after the binding of subgroup I inhibitors, but becomes fixed after the binding of subgroup II inhibitors. Stigmatellin formed a hydrogen bond with ISP, so it is very easy to understand why it holds the ISP in a fixed position.[4] However, unlike stigmatellin, famoxadone do not make a hydrogen bond (or any direct contact of any kind) with the ISP, and thus it is somewhat of a mystery how famoxadone fix the ISP. Therefore, it has been proposed that the mechanism by which inhibitors control the position of the ISP is likely to be related to mechanism of enforcement of the bifurcated reaction at Q_o site.[2,4,6]

Famoxadone, 5-methyl-5-(4-phenoxyphenyl)-3-(phenylamino)-2,4-oxazolidinedione, is a new agricultural fungicide discovered by the collaboration between DuPont and the Geffken research group at University of Bonn, Germany.[7] It is a member of a new class of oxazolidinedione fungicides which belong to the bc_1 complex Q_oI family. However, site mutations at the bc_1 complex have resulted in an explosive increase in resistance

* Corresponding authors.
E-mail addresses: jiaweiwu@mail.tsinghua.edu.cn (J.-W. Wu), gfyang@mail.ccnu.edu.cn (G.-F. Yang).
[1] Co-first authors.

0968-0896/$ - see front matter © 2011 Elsevier Ltd. All rights reserved.
doi:10.1016/j.bmc.2011.06.008

associated with Q_oI fungicides.[8–10] The resistance of the bc_1 complex to famoxadone developed much slower than resistance to the methoxyacrylate(MOA)-type inhibitors like azoxystrobin and kresoxim-methyl.[10–12] Therefore, the design and syntheses of oxazolidinedione derivatives have attracted much attention from the synthetic chemists with the aim of discovering novel fungicides with both high potency and low risk of resistance.[13,14]

Oxazolidinedione-type Q_oI fungicides have the common structural feature of a 3,5,5-trisubstituted oxazolidinedione (Fig. 1). Studies of the structure–activity relationship indicated that the R^1 and R^3 groups were sensitive to structural variation, whereas compounds with a wide variety of R^2 groups were fungicidally active. The optimal group at the R^2 position was the phenoxyphenyl group. However, the earlier structure–activity relationships were established according to results of in vivo fungicidal activity.[7] Although the crystal structure of mitochondrial cytochrome bc_1 in complex with famoxadone has been determined,[15] the substituent effects of oxazolidinedione derivatives on the inhibitory activity against the bc_1 complex remain unclear. Therefore, to understand the detailed mechanism of the interaction between the oxazolidinedione-type inhibitors and the bc_1 complex, we designed and synthesized a series of oxazolidinedione derivatives **4a–k** ($R^1 = CH_3$; R^2 = 6-bromopyridin-3-yl; R^3 = various substituted phenylamino) and **8a–k** ($R^1 = CH_3$; R^2 = phenoxyphenyl; R^3 = various substituted phenylamino). Herein, we present the results of the inhibition activities against the porcine bc_1 complex and discuss the structure-activity relationships of these newly synthesized compounds. Moreover, the X-ray diffraction of bc_1 complex with bound famoxadone[15] indicated that it belongs the family of Q_o site inhibitors, but famoxadone has been reported as a non-competitive inhibitor of bc_1 complex with respect to the substrate QH_2.[16] This earlier kinetic result does not seem to be feasible because inhibitors binding to the same pocket as the substrate should be competitive. We speculated that this earlier study was likely not to take the non-enzymatic oxidation of QH_2 into consideration, a process that our previous work showed has significant influence on the kinetic behavior.[17] Therefore, we undertook a detailed investigation of the inhibitory kinetics of famoxadone and the representative compound (**8d**) against the porcine bc_1 complex with respect to the substrates of cytochrome *c* and DBH_2. The results showed clearly that famoxadone and compound **8d** are both non-competitive inhibitors with respect to substrate cytochrome *c*, but are competitive inhibitors with respect to substrate DBH_2.

2. Results and discussion

2.1. Synthetic chemistry of the title compounds

The synthetic route for compound **4a–k** is shown in Scheme 1. Due to the strong electron-withdrawing ability of the nitrogen atom, it is very difficult for 2,5-dibromopyridine **1** to react with magnesium to afford a Grignard reagent. Therefore, 2,5-dibromopyridine was firstly converted to the Grignard reagent of (6-bromopyridin-3-yl)-magnesium chloride **2** via a procedure of halogen-magnesium exchange. By controlling the conditions, the reaction took place selectively at position 5 of the pyridine ring and only one product was obtained. Then, the THF solution of the Grignard reagent **2** reacted with a cooled (−78 °C) solution of ethyl pyruvate to afford the key intermediate of ethyl 2-(6-bromopyridin-3-yl)-2-hydroxyl-propanoate **3**. Finally, compound **3** was reacted with 1,1′-carbonyldiimidazole (CDI) to form the intermediate acylimidazole. Without isolation, the obtained acylimidazole was subjected to a one-pot reaction with various substituted phenylhydrazines and acetic acid (HOAc) to give the target compounds **4** with isolated yields of 25–69%. The phenylhydrazine bearing an electron-withdrawing group, for example, CF_3, NO_2, always resulted in low yields of products, while those phenylhydrazines bearing electron-donating groups, for example, 4-OCH_3, 2,4-$(CH_3)_2$, always resulted in relative high yields of products. In addition, acetic acid is critical to the one-pot reaction. If acetic acid was omitted, no product was obtained. As shown in Scheme 2, compounds **8a–k** was prepared according to a similar procedure as the preparation of compounds **4a–k** in yields of 36–57%. The difference is that 1-bromo-4-phenoxybenzene **5** can react smoothly with magnesium to afford Grignard reagent **6**, whereas 2,5-dibromopyridine **1** needs to undergo halogen-magnesium exchange. The structures of all intermediates and title compounds were confirmed by ^{1}H NMR and HRMS spectral data.

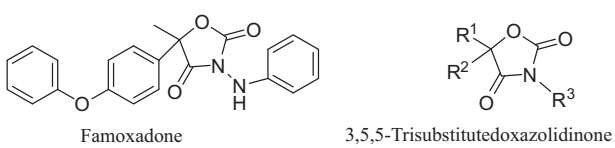

Figure 1. Chemical structures of famoxadone and 3,5,5-trisubstituted oxazolidinedione.

2.2. Inhibition activities of compounds 4a–k and 8a–k against porcine succinate–cytochrome *c* reductase (SCR)

SCR is the mixture of respiratory complex II and the bc_1 complex (complex III), which was also deemed to form complex II–complex III supercomplexes.[18] Complex II (SQR) firstly passes electrons from succinate to ubiquinone, and then the cytochrome bc_1 complex passes electrons from reduced ubiquinone to cytochrome *c*. The activity of complex II in SCR was selectively determined using succinate and dichlorophenolindophenol (DCIP) as substrates, and the activity of only the cytochrome bc_1 complex in SCR was determined using decylubiquinol (DBH_2) and cytochrome *c* as substrates, whereas the overall activity of SCR (both complex II and bc_1 complex) was determined using succinate and cytochrome *c* as substrates.

The results indicated that all of the compounds exhibited no effect on the activity of complex II (data not shown), but markedly inhibited the activities of the bc_1 complex and SCR. The IC_{50} values of compounds **4a–k** and **8a–k** against SCR from porcine heart mitochondria (in Table 1) show that although the potency of the newly synthesized compounds was not superior to famoxadone, some interesting structure–activity relationships are evident. Compounds **4a–k** always showed very low inhibition activities against SCR, suggesting that the phenoxyphenyl group is critical to maintain high potency. The X-ray diffraction of bc_1 complex with bound famoxadone indicated that the *van der Waals* interactions between the phenoxyphenyl group and hydrophobic residues M124, F128, I146, P270, Y273, F274, Y278, and I298, made great contributions to the binding of famoxadone.[15] The 2-bromopyridyl group ($C\log P = 1.59$) is more hydrophilic than the phenoxyphenyl group ($C\log P = 4.24$), resulting in a notable reduction in the *van der Waals* interactions between the 2-bromopyridyl group and the above hydrophobic residues. The greater hydrophobic interactions also account for the higher inhibitory activity of compounds **8a–k** as compared to compounds **4a–k**. However, the substituents on the phenylamino group have great effects on the inhibition activity. According to the results of X-ray diffraction analysis,[15] the phenylamino group of famoxadone was located deep inside the Q_o pocket and interacted with hydrophobic residues M138, G142, V145, I146, I268, P270, and Y278, of which V145, I268, and Y278 are part of the iron–sulfur protein (ISP) docking crater. Therefore, a hydrophobic group (4-Br, 4-Cl and 4-CH_3) at this site is favorable, whereas an electron-withdrawing group (4-COOH, 4-CN and

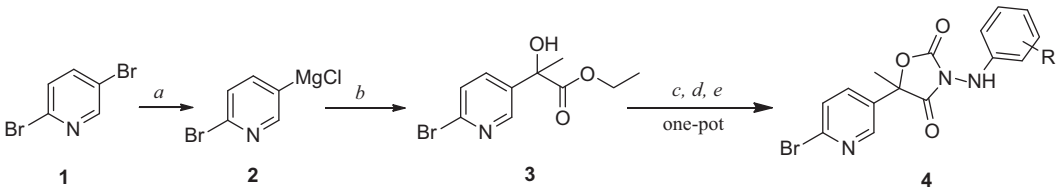

Scheme 1. Synthesis of 5-(6-bromopyridin-3-yl)-5-methyl-3-(phenylamino)oxazolidine-2,4-diones **4a**–**k**. Reagents and conditions: *a*, *i*-PrCl, Mg, I_2, THF, reflux; *b*, ethyl pyruvate, −78 °C, THF; *c*, CDI, 25 °C, CH_2Cl_2; *d*, H_2O, HOAc, rt; *e*, substituted phenylhydrazine, CH_2Cl_2, rt.

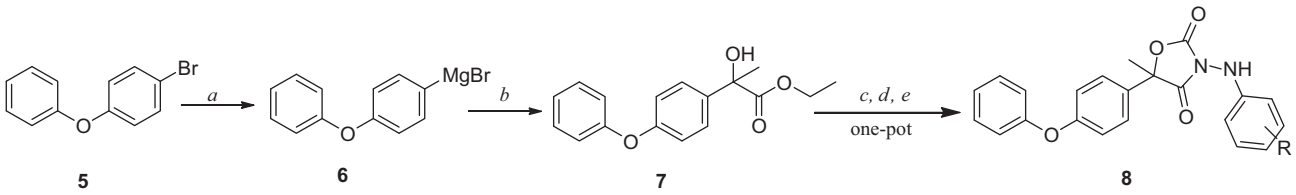

Scheme 2. Synthesis of 5-methyl-5-(4-phenoxyphenyl)-3-(phenylamino)oxazolidine-2,4-diones **8a**–**k**. Reagents and conditions: *a*, Mg, I_2, THF, reflux; *b*, ethyl pyruvate, −78 °C, THF; *c*, CDI, 25 °C, CH_2Cl_2; *d*, H_2O, HOAc, rt; *e*, substituted phenylhydrazine, CH_2Cl_2, rt.

Table 1
The inhibitory activities of compounds **4a**–**k** and **8a**–**k** against porcine SCR

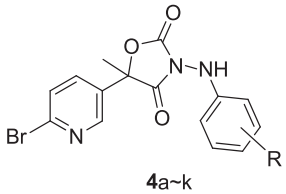

4a~k

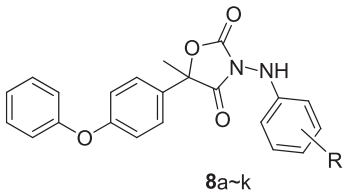

8a~k

No.	R	IC_{50}[a] (nM)	No.	R	IC_{50}[a] (nM)
4a	H	>1000	**8a**	3-COOH	24.04
4b	2-Br-4-F	>1000	**8b**	2-Br-4-F	59.98
4c	2,6-$(CH_3)_2$	>1000	**8c**	2,6-$(CH_3)_2$	1516.92
4d	4-Br	>1000	**8d**	4-Br	9.44
4e	4-CF_3	>1000	**8e**	4-CF_3	63.26
4f	4-CN	>1000	**8f**	4-CN	275.17
4g	4-CH_3	>1000	**8g**	4-CH_3	23.76
4h	4-Cl	>1000	**8h**	4-Cl	18.79
4i	4-OCH_3	>1000	**8i**	4-OCH_3	57.92
4j	2,4-$(CH_3)_2$	>1000	**8j**	2,4-$(CH_3)_2$	15.93
4k	4-NO_2	>1000	**8k**	4-COOH	5312.08
			Famoxadone		3.62

[a] Determined with the substrate of cytochrome *c*.

4-CF_3) would be unfavorable. For example, compound **8d** (R = 4-Br) exhibited relatively high inhibition, while compound **8k** (R = 4-COOH) showed 563-times lower activity than compound **8d** (Table 1). In addition, the conformation of the phenylamino group is very important for the binding. If the substituents affected the conformation of the phenylamino group, the inhibitory activity will greatly reduced. For example, compound **8c** is 419-times less potent than famoxadone due to its 2,6-dimethyl substitution pattern.

2.3. Inhibitory kinetics of 8d and famoxadone

In order to understand the mechanism by which these compounds inhibit this electron transport complex, we further studied the inhibitory kinetics of **8d** against SCR and also selectively examined the effects on only the bc_1 complex. SCR catalyzed the overall electron transfer from succinate to the water-soluble electron acceptor cyt. *c*. As shown in Figure 2A, double-reciprocal plots showed non-competitive inhibition of **8d** with respect to cyt. *c*. Furthermore, we examined the effect of **8d** on the reactions of the SCR pathway catalyzed by the bc_1 complex. We determined the kinetics of the bc_1 complex activity with respect to the substrate ubiquinol by using the artificial electron donor decylubiquinol (DBH_2) and cytochrome *c* as substrates in the absence and presence of **8d**. As shown in Figure 2B, **8d** competitively inhibited that portion of SCR activity catalyzed by the bc_1 complex in a competitive manner with respect to the substrate DBH_2. These results indicate that **8d** binds to the same hydrophobic binding pocket as the ubiquinol-binding site. It is consistent with some X-ray structures of bc_1 complex in which this type of inhibitor binds to the Q_o site of the bc_1 complex.[4] A similar result was obtained for the commercial fungicide famoxadone. As shown in Figure 2C and D, famoxadone is a non-competitive inhibitor (K_i = 3.62 nM) with respect to the substrate of cytochrome *c*, but is a competitive inhibitor (K_i = 51.43 nM) with respect to the substrate of DBH_2. It is well known that most of the quinol analogs are readily autooxidized, thus producing both superoxide and hydrogen peroxide which can ultimately lead to reduction of cytochrome *c*, resulting in an exchange of electrons indirectly with cytochrome *c* in solution.[19] Therefore, it is very important to minimize the nonenzymatic oxidation of the quinol substrate when assaying the bc_1 complex activity.[19] In contrast to earlier studies,[16] we added the nonionic detergent lauryl maltoside to prevent the nonenzymatic oxidation of DBH_2. The nonenzymatic rate for cytochrome *c* reduction in our experiment was followed for at least 100 s before the enzyme was added to initiate the reaction for each study. In our data analysis, we subtracted the rate of the nonenzymatic activity from the overall reaction rate. In earlier investigations performed by other workers,[15] reduced quinone was added into the enzyme solution to start the reaction. As a result, the nonenzymatic and enzymatic reactions could not be distinguished. Famoxadone can only inhibit the enzyme catalyzed transfer of electrons to cytochrome *c* and the contribution of the nonenzymatic reaction led other investigators to conclude that famoxadone is a non-competitive inhibitor of the bc_1 complex with respect to the substrate QH_2, an analog of DBH_2. In addition, Figure 2E and F clearly indicated that azoxystrobin is a non-competitive inhibitor (K_i = 295.10 nM) with respect to the substrate of cytochrome *c*, but is a competitive inhibitor (K_i = 204.20 nM) with respect to the substrate of DBH_2.

We compared the inhibitory activities of three inhibitors against porcine SCR and the bc_1 complex (Figure 2 and Table 2). Compound **8d** and famoxadone exhibited, respectively, 35-fold

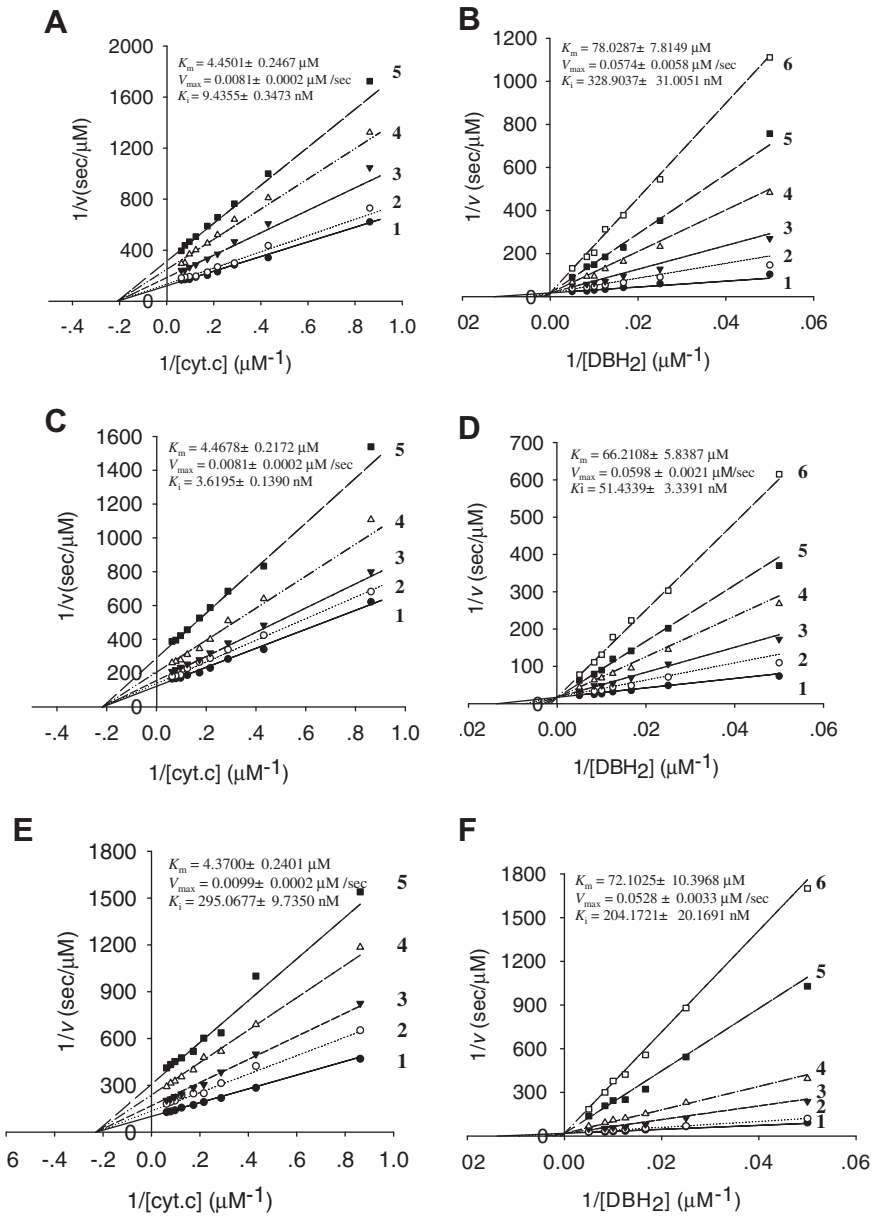

Figure 2. Kinetic analysis of inhibition by **8d** (A and B), famoxadone (C and D) and azoxystrobin (E and F). The inhibition of porcine SCR by (A) **8d** (1, 0 nM; 2, 1 nM; 3, 5 nM; 4, 10 nM and 5, 15 nM), (C) famoxadone (1, 0 nM; 2, 0.5 nM; 3, 1 nM; 4, 2.5 nM and 5, 5 nM) and (E) azoxystrobin (1, 0 nM; 2, 100 nM; 3, 200 nM; 4, 400 nM and 5, 600 nM). Each reaction mixture contains 100 mM PBS (pH 7.4), 0.3 mM EDTA, 20 mM succinate, 0.1 nM enzyme, 1.16–16.02 μM cytochrome *c* and the indicated amount of **8d**, famoxadone or azoxystrobin. By assuming non-competitive inhibition, K_m (cyt. *c*), V_{max}, and K_i were estimated. The inhibition of porcine bc_1 complex by (B) **8d** (1, 0 nM; 2, 500 nM; 3, 1000 nM; 4, 2000 nM; 5, 3000 nM; and 6, 5000 nM), (D) famoxadone (1, 0 nM; 2, 50 nM; 3, 100 nM; 4, 200 nM; 5, 300 nM; and 6, 500 nM) and (F) azoxystrobin (1, 0 nM; 2, 100 nM; 3, 500 nM; 4, 1000 nM; 5, 3000 nM; and 6, 5000 nM). Each reaction mixture contains 100 mM PBS (pH 7.4), 0.3 mM EDTA, 750 μM lauryl maltoside, 100 μM oxidized cytochrome *c*, 0.1 nM SCR, 20–200 μM DBH_2 and the indicated amount of **8d**, famoxadone or azoxystrobin. By assuming competitive inhibition, K_m (DBH_2), V_{max}, and K_i were also estimated.

Table 2
The inhibition effect of some inhibitors against porcine SCR and bc_1 complex

Inhibitor	SCR (Succinate–cyt.c system 23 °C)			bc_1 complex (DBH_2–cyt.c system 23 °C)			
	IC_{50}[a] (nM)	Inhibition type (with cyt.c)	K_i[a] (nM)	IC_{50} without LM[a] (nM)	IC_{50} with LM[b] (nM)	Inhibition type (with DBH_2)	K_i[b] (nM)
8d	9.03	Non-competitive	9.44 ± 0.35	337.13	1049.32	Competitive	328.9 ± 31.0
Famoxadone	4.78	Non-competitive	3.62 ± 0.14	48.21	142.02	Competitive	51.43 ± 3.34
Azoxystrobin	291.30	Non-competitive	295.10 ± 9.74	434.71	527.12	Competitive	204.2 ± 20.2

[a] Reaction buffer: 100 mM PBS (pH 7.4), 0.3 mM EDTA.
[b] Reaction buffer: 100 mM PBS (pH 7.4), 0.3 mM EDTA, 750 μM lauryl maltoside (*n*-dodecyl-β-D-maltoside).

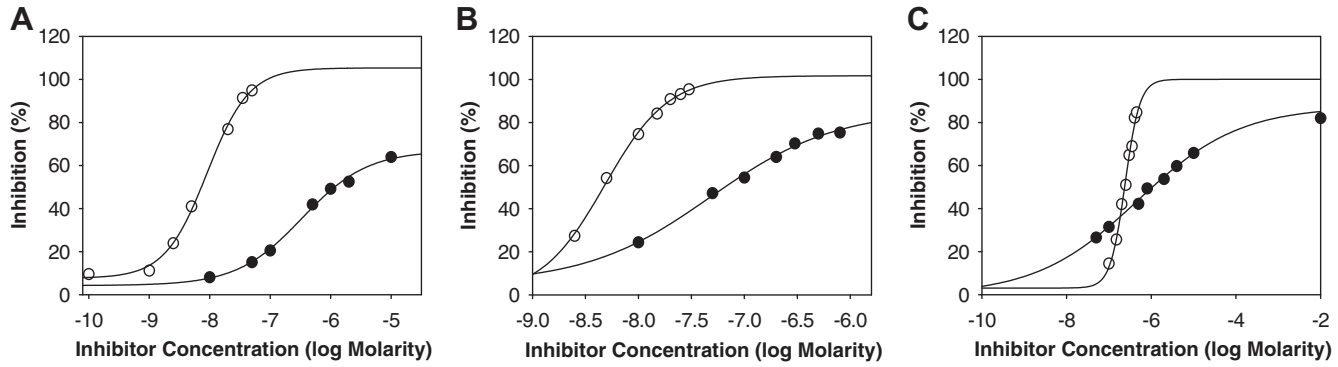

Figure 3. The inhibition of SCR and QCR activities of porcine SCR by **8d** (A), famoxadone (B) and azoxystrobin (C). Open circles (SCR activity): each reaction mixture contains 100 mM PBS (pH 7.4), 0.3 mM EDTA, 20 mM succinate, 0.1 nM enzyme, 60 μM cytochrome *c* and the indicated amount of inhibitors. Solid circles (QCR activity): each reaction mixture contains 100 mM PBS (pH 7.4), 0.3 mM EDTA, 100 μM DBH_2, 0.1 nM enzyme, 100 μM cytochrome *c* and the indicated amount of inhibitors.

and 15-fold greater inhibition against the porcine SCR than against the porcine bc_1 complex, as indicated by the K_i values. We also found that compound **8d** and famoxadone did not show inhibitory effects against complex II at concentrations as high as 20 μM (data not shown). Furthermore, we also measured the IC_{50} values of the three inhibitors with respect to the bc_1 complex in the absence and presence of the nonionic detergent lauryl maltoside. The differences in IC_{50} values were retained even when the same reaction buffer was used both in the succinate–cyt. *c* system and DBH_2–cyt. *c* system. Figure 3 shows that the inhibition ability of compound **8d** and famoxadone decreased more than ten times while that for azoxystrobin decreased only by half when measuring bc_1 complex activity with DBH_2 and cyt. *c* as substrates. The reason for the inhibition decline may be attributed to the use of DBH_2. When DBH_2 was used as substrate to measure the bc_1 complex activity, the V_{max} of the bc_1 complex was seven-fold higher than that of SCR. Thus, we had to increase the concentration of inhibitors to achieve the same degree of inhibition. For example, when we determined the K_i values of famoxadone in these two systems, we set the inhibitor concentrations of 0–5 nM for measuring SCR activity but concentrations ranging from 0 to 500 nM were required for inhibiting the bc_1 complex activity. Of course, both the competitive effect of substrate in the high quinol concentration and the effect of detergent will lead to high IC_{50} values, but difficulties in doing kinetic experiments with water-insoluble substrates and inhibitors, makes it difficult to prove. Furthermore, a recent report[20] has showed that decylubiquinone (DB) can increase the activities of complex I/III and complex II/III, attenuate reductions in oxygen consumption at high concentrations of the complex III inhibitor, and induce increases in mitochondrial function in the nerve terminal during complex I or III inhibition. Our experimental results also indicated that DBH_2 had some similar features as DB.

It is well known that the rate-limiting step will control the overall reaction process when considering the overall rate of an enzyme sequence. The difference in rates between SCR and bc_1 suggest that the rate limiting step is before the bc_1 complex. This rate-limiting step may be most sensitive to these inhibitors, as indicated by the lower K_i values when the SCR is measured. Therefore, we proposed that these two inhibitors not only inhibited the activity of the bc_1 complex, but also might affect the interaction between the complex II and the bc_1 complex. In fact, earlier biophysical investigations have suggested the existence of a complex II-complex III pro-supercomplex, although to date this supercomplex has not been isolated.[21,22] When we prepared the protein from porcine heart, we found it is easier for co-purification of complex II–complex III (SCR) with excellent quality and activity. Another report showed no evidence for association of complex-II with anything by blue native-polyacrylamide gel electrophoresis,[23] but a further analysis of the exothermic enthalpy change of thermodenaturation of a protein-phospholipid vesicle containing both complex II and complex III also suggested the presence of a specific interaction between complexes II and III.[24] However, no reports have indicated that a small molecule can interfere with the interaction between complex II and III. Interestingly, in contrast to compound **8d** and famoxadone, azoxystrobin (AZ) inhibited the SCR and the bc_1 complex with similar K_i values (Figure 2E, 2F and Table 2). The above results indicated that although all three compounds belong to the family of Q_o-specific inhibitors, 3-(phenylamino)-oxazolidine-2,4-dione derivatives (such as famoxadone and compound **8d**) and methoxyacrylate-type derivatives (such as AZ) should have different mechanisms of biological action. This phenomenon might also account for why famoxadone showed lower prevalence of resistance than methoxyacrylate-type Q_o-specific inhibitors.

It has been established that the ISP domain has a dynamic role in the electron transfer between cytochrome *b* and c_1 by functioning as a tethered, but flexible shuttle between the two redox centers. The ISP is held in a fixed position close to cytochrome *b* when famoxadone is bound, whereas it becomes mobilized when AZ is bound. The flexibility of the ISP domain is required for electron flow in the high-potential chain. Although famoxadone and AZ occupy overlapping regions in the Q_o pocket, they do exhibit different characteristics according to their different binding modes with the ISP domain, which was further confirmed by our experimental results. We therefore speculate that oxazolidinedione derivatives such as famoxadone and our novel compound **8d** possibly block the interaction between complexes II and III by fixing the ISP domain.

3. Conclusion

In summary, a series of new oxazolidinedione derivatives were designed and synthesized as potent inhibitors against the cytochrome bc_1 complex. Based on the results of the inhibition activities against porcine bc_1 complex, the structure–activity relationships of these newly synthesized compounds were discussed. Detailed investigation of the effect of the inhibitors on the steady state kinetics revealed that the representative compound **8d** and famoxadone are both non-competitive inhibitors with respect to the substrate cytochrome *c*, but competitive inhibitors with respect to the substrate DBH_2. In addition, com-

pound **8d** and famoxadone showed, respectively, 35-fold and 15-fold greater inhibitory activity against the porcine SCR than against the porcine bc_1 complex, indicating that these two inhibitors not only inhibited the activity of the bc_1 complex, but possibly interfered with the interaction between the complex II and the bc_1 complex. To our knowledge, this is the first report that famoxadone and its analogs might affect the interaction between the complex II and the bc_1 complex.

4. Materials and methods

4.1. Reagents and equipment

Unless otherwise noted, all chemical reagents were commercially available and treated with standard methods before use. Silica gel column chromatography (CC): silica gel (200–300 mesh); Qingdao Makall Group Co., Ltd; Qingdao; China). Solvents were dried in a routine way and redistilled. ^{1}H spectra were recorded in $CDCl_3$ or DMSO-d_6 on a Varian Mercury 600 or 400 spectrometer and resonances (δ) are given in ppm relative to tetramethylsilane (TMS). The following abbreviations were used to designate chemical shift mutiplicities: s = singlet, d = doublet, t = triplet, m = multiplet, br = broad. High resolution mass spectra (HRMS) were acquired in positive mode on a WATERS MALDI SYNAPT G2 HDMS(MA, USA) or an Agilent 6520 Accurate-Mass Q-TOF liquid chromatography/mass spectrometry (LC/MS)(USA). Melting points were taken on a Buchi B-545 melting point apparatus and are uncorrected.

4.2. Synthesis of the intermediate 3[25–27]

Under a nitrogen atmosphere, *i*-propyl chloride (780 mg, 10 mmol) was added dropwise to a mixture of Mg (288 mg, 12 mmol) and a small amount of iodine in anhydrous THF (10 mL). After refluxing for 2 h, 2,5-dibromopyridine (2.36 g, 10 mmol) was added slowly. Then, the resulting mixture was stirred for 2.5 h at 70 °C, and cooled to room temperature to afford the intermediate of Grignard reagent **2**, which was dissolved in THF and added dropwise to a cooled (−78 °C) solution of ethyl pyruvate (1.16 g, 10 mmol). After completion of the addition, the reaction temperature was slowly allowed to warm to 20 °C and kept overnight. The reaction mixture was poured into an ice solution of HCl and then extracted with methylene chloride (3 × 40 mL). The methylene chloride extract was washed with brine (30 mL) and dried with $MgSO_4$. Evaporation of methylene chloride at reduced pressure afforded the crude product. After purification by flash column chromatography, the intermediate **3** (1.64 g) was obtained as a pale yellow oil in a yield of 60%. ^{1}H NMR (600 MHz, $CDCl_3$): δ 1.28 (t, J = 6.9 Hz, 1H, CH_3), 1.78 (s, 3H, CH_3), 3.99 (s, 1H, OH), 4.23–4.30 (m, 2H, CH_2), 7.47 (d, J = 8.4 Hz, 1H, Py-H), 7.79 (d, J = 8.4 Hz, 1H, Py-H), 8.59 (s, 1H, Py-H).

4.3. General procedures for the preparation of target compounds 4a–k[7,28–30]

A mixture of ethyl 2-(6-bromopyridin-3-yl)-2-hydroxypropanoate (**3**, 4 mmol), 1,1′-carbonyldiimidazole (CDI) (5 mmol) and dry dichloromethane (15 mL) was stirred at 25 °C for 24 h. When the reaction was completed, as monitored by TLC detection, 8 mL of water was then added and the mixture was stirred for a further 15 min. Then, acetic acid (3 mL) and the substituted phenylhydrazine (5.32 mmol) were then added, and the obtained mixture was stirred at 25 °C for 26 h. After the reaction was completed, as evidenced by TLC detection, 30 mL of water was added and the pH value of the solution was adjusted to about 2 with HCl. Then, the organic layer was separated and the aqueous layer was extracted twice with methylene chloride. The combined organic phases were dried with $MgSO_4$ and evaporated at reduced pressure to obtain the crude product, which was then purified by flash column chromatography to give the pure products in yields of 25–69%.

4.3.1. Data for 4a

White solid, yield 68%, mp 144–145 °C. ^{1}H NMR(600 MHz, $CDCl_3$): δ 2.01(s, 3H, Het–CH_3), 6.09 (s, 1H, NH), 6.74 (d, J = 7.8 Hz, 1H, ArH), 7.04 (t, J = 7.2 Hz, 1H, ArH), 7.26–7.29 (m, 2H, ArH), 7.59 (d, J = 8.4 Hz, 1H, Py-H), 7.81 (dd, J = 3.6 and 8.4 Hz, 1H, Py-H), 8.65 (d, J = 7.8 Hz, 1H, Py-H); HRMS(MALDI): Calcd for $C_{15}H_{12}BrN_3O_3$ $[M+H]^+$ 362.0153. Found: 362.0140.

4.3.2. Data for 4b

White solid, yield, 61%, mp 143–144 °C. ^{1}H NMR(600 MHz, $CDCl_3$): δ 2.01 (s, 3H, Het–CH_3), 6.49 (dd, J = 4.8 and 9.6 Hz, 1H, ArH), 6.54 (s, 1H, NH), 6.95 (s, 1H, ArH), 7.30 (dd, J = 2.4 and 7.8 Hz, 1H, ArH), 7.59 (d, J = 8.4 Hz, 1H, Py-H), 7.80 (dd, J = 2.4 Hz and J = 8.4 Hz, 1H, Py-H), 8.64 (d, J = 2.4 Hz, 1H, Py-H); HRMS(MALDI): Calcd for $C_{15}H_{10}Br_2FN_3O_3$ $[M+H]^+$ 457.9149. Found: 457.9151.

4.3.3. Data for 4c

White solid, yield, 53%, mp 134–135 °C. ^{1}H NMR(600 MHz, $CDCl_3$): δ 2.33 (s, 3H, Het–CH_3), 2.42 (s, 6H, Ar-2×CH3), 6.07 (s, 1H, NH), 6.77 (s, 1H, ArH), 6.92 (s, 1H, ArH), 7.00 (s, 1H, ArH), 7.03(s, 1H, Py-H), 7.20 (s, 1H, Py-H), 8.09(s, 1H, Py-H); HRMS(MALDI): Calcd for $C_{17}H_{16}BrN_3O_3$ $[M+Na]^+$ 412.0154. Found: 412.0273.

4.3.4. Data for 4d

White solid, yield, 25%, mp 177–178 °C. ^{1}H NMR (600 MHz, $CDCl_3$): δ 2.00(s, 3H, Het–CH_3), 6.08 (s, 1H, NH), 6.64 (t, J = 8.2 Hz, 2H, ArH), 7.38 (d, J = 8.8 Hz, 2H, ArH), 7.59 (d, J = 8.0 Hz, 1H, Py-H), 7.78 (dd, J = 2.4 and 8.0 Hz, 1H, Py-H), 8.64 (d, J = 2.4 Hz, 1H, Py-H); HRMS(MALDI): Calcd for $C_{15}H_{11}Br_2N_3O_3$ $[M+H]^+$ 439.9227. Found: 439.9245.

4.3.5. Data for 4e

White solid, yield, 58%, mp 151–152 °C. ^{1}H NMR(600 MHz, $CDCl_3$): δ 2.03 (s, 3H, Het–CH_3), 6.34 (s, 1H, NH), 6.76 (d, J = 9.0 Hz, 2H, ArH), 7.53 (d, J = 8.4 Hz, 2H, ArH), 7.60 (d, J = 9.0 Hz, 1H, Py-H), 7.81 (dd, J = 2.4 and 8.4 Hz, 1H, Py-H), 8.65 (d, J = 2.4 Hz, 1H, Py-H); HRMS(MALDI): Calcd for $C_{16}H_{11}BrF_3N_3O_3$ $[M+H]^+$ 430.0008. Found: 430.0014.

4.3.6. Data for 4f

White solid, yield, 69%, mp 183–184 °C. ^{1}H NMR(400 MHz, $CDCl_3$): δ 2.04 (s, 3H, Het–CH_3), 6.37 (s, 1H, NH), 6.73 (d, J = 8.4 Hz, 2H, ArH), 7.57–7.62 (m, 3H, ArH and Py-H), 7.81 (dd, J = 2.4 and 8.4 Hz, 1H, Py-H), 8.65 (d, J = 2.4 Hz, 1H, Py-H); HRMS(MALDI): Calcd for $C_{16}H_{11}BrN_4O_3$ $[M+H]^+$ 387.0101. Found: 387.0093.

4.3.7. Data for 4g

White solid, yield, 48%, mp 162–163 °C. ^{1}H NMR(600 MHz, $CDCl_3$): δ 1.99 (s, 3H, Het–CH_3), 2.28 (s, 3H, Ar-CH_3), 5.97 (s, 1H, NH), 6.69 (d, J = 8.4 Hz, 2H, ArH), 7.07 (d, J = 8.4 Hz, 2H, ArH), 7.57 (d, J = 8.4 Hz, 1H, Py-H), 7.79 (dd, J = 2.4 and 9.0 Hz, 1H, Py-H), 8.64 (d, J = 3.0 Hz, 1H, Py-H); HRMS(MALDI): Calcd for $C_{16}H_{14}BrN_3O_3$ $[M+H]^+$ 376.0272. Found: 376.0297.

4.3.8. Data for 4h

White solid, yield, 51%, mp 160–161 °C. ^{1}H NMR(400 MHz, $CDCl_3$): δ 2.00 (s, 3H, Het–CH_3), 6.10 (s, 1H, NH), 6.69 (t, J = 4.2 Hz, 2H, ArH), 7.24 (t, J = 4.2 Hz, 2H, ArH), 7.59 (d,

J = 8.4 Hz, 1H, Py-H), 7.78 (t, J = 5.6 Hz, 1H, Py-H), 8.633 (d, J = 2.4 Hz, 1H, Py-H); HRMS(MALDI): Calcd for $C_{15}H_{11}BrClN_3O_3$ $[M+H]^+$ 395.9752. Found: 395.9751.

4.3.9. Data for 4i

White solid, yield, 49%, mp 129–130 °C. ^{1}H NMR(400 MHz, $CDCl_3$): δ 1.97 (s, 3H, Het–CH_3), 3.76 (s, 3H, Ar–OCH_3), 5.95 (s, 1H, NH), 6.80–6.86 (m, 4H, ArH), 7.57 (d, J = 8.8 Hz, 1H, Py-H), 7.79 (t, J = 3.0 Hz, 1H, Py-H), 8.62 (d, J = 2.4 Hz, 1H, Py-H); HRMS(MALDI): Calcd for $C_{16}H_{14}BrN_3O_4$ $[M+H]^+$ 392.0268. Found: 392.0246.

4.3.10. Data for 4j

White solid, yield, 52%, mp 142–143 °C. ^{1}H NMR(400 MHz, $CDCl_3$): δ 2.00 (s, 3H, Het–CH_3), 2.24 (s, 3H, Ar-CH_3), 2.30 (s, 3H, Ar-CH_3), 5.92 (s, 1H, NH), 6.40 (d, J = 8.4 Hz, 1H, ArH), 6.89 (d, J = 8.8 Hz, 1H, ArH), 6.96 (s, 1H, ArH), 7.57 (d, J = 8.4 Hz, 1H, Py-H), 7.81 (t, J = 4.4 Hz, 1H, Py-H), 8.64 (d, J = 2.8 Hz, 1H, Py-H); HRMS(MALDI): Calcd for $C_{17}H_{16}BrN_3O_3$ $[M+H]^+$ 390.0444. Found: 390.0453.

4.3.11. Data for 4k

White solid, yield, 42%, mp 92–93 °C. ^{1}H NMR(400 MHz, $CDCl_3$): δ 2.05 (s, 3H, Het–CH_3), 6.44 (s, 1H, NH), 6.74 (d, J = 8.4 Hz, 2H, ArH), 7.62 (d, J = 8.8 Hz, 1H, Py-H), 7.80 (t, J = 5.6 Hz, 1H, Py-H), 8.19(d, J = 9.6 Hz, 2H, ArH), 8.66 (d, J = 2.4 Hz, 1H, Py-H); HRMS(MALDI): Calcd for $C_{15}H_{11}BrN_4O_5$ $[M+H]^+$ 406.9988. Found: 406.9991.

4.4. Synthesis of intermediate 7[26,27]

A THF solution (15 mL) of 1-bromo-4-phenoxybenzene (2.48 g, 10 mmol) was added dropwise to a mixture of Mg (288 mg, 12 mmol) and a small amount of iodine in anhydrous THF (10 mL). After refluxing for 1 h, the Grignard reagent of (4-phenoxyphenyl)magnesium bromide was obtained, which was dissolved in THF and added dropwise to a cooled (−78 °C) solution of ethyl pyruvate (1.16 g, 10 mmol). After completion of the addition, the reaction temperature was slowly allowed to rise to 20 °C and kept overnight. The reaction mixture was poured into an ice solution of HCl and then extracted with methylene chloride (3 × 40 mL). The methylene chloride extract was washed with brine (30 mL) and dried with $MgSO_4$. Evaporation of methylene chloride at reduced pressure afforded the crude product. After purification by flash column chromatography, the intermediate **7** (1.49 g) was obtained as a pale yellow oil in a yield of 52%. ^{1}H NMR (600 MHz, $CDCl_3$): δ 1.27 (t, J = 7.2 Hz, 1H, CH_3), 1.77 (s, 3H, CH_3), 3.78 (s, 1H, OH), 4.22–4.27 (m, 2H, CH_2), 6.97 (d, J = 9.0 Hz, 2H, ArH), 7.01 (d, J = 7.8 Hz, 2H, ArH), 7.11 (t, J = 7.5 Hz, 1H, ArH), 7.34 (t, J = 7.8 Hz, 2H, ArH), 7.51 (d, J = 8.4 Hz, 2H, ArH).

4.5. General procedures for the preparation of target compounds 8a–k

According to the similar procedure as for the preparation of compounds **4a–k**, compounds **8a–k** was prepared in yields of 36–57%.

4.5.1. Data for 8a

White solid, yield, 49%, mp 148–149 °C. ^{1}H NMR(400 MHz, DMSO): δ 2.03 (s, 3H, Het–CH_3), 6.75 (d, J = 7.8 Hz, 2H, ArH),7.07 (d, J = 8.4 Hz, 2H, ArH), 7.11 (d, J = 8.4 Hz, 2H, ArH), 7.20 (s, 1H, ArH), 7.26 (d, J = 8.4 Hz, 2H, ArH), 7.43 (d, J = 7.5 Hz, 2H, ArH), 7.55 (d, J = 7.8 Hz, 2H, ArH), 8.84 (s, 1H, NH); HRMS(MALDI): Calcd for $C_{23}H_{18}N_2O_6$ $[M+Na]^+$ 441.0118. Found: 441.1063.

4.5.2. Data for 8b

White solid, yield, 36%, mp 144–145 °C. ^{1}H NMR(600 MHz, $CDCl_3$): δ 2.00 (s, 3H, Het–CH_3), 6.48 (s, 1H, NH), 6.50 (dd, J = 5.4 Hz, J = 9.0 Hz, 1H, ArH), 6.93 (t, J = 8.4 Hz, 1H, ArH), 7.04 (t, J = 6.6 Hz, 4H, ArH), 7.17 (t, J = 7.2 Hz, 1H, ArH), 7.29 (d, J = 7.8 Hz, 1H, ArH), 7.38 (t, J = 7.5 Hz, 2H, ArH), 7.53 (d, J = 8.4 Hz, 2H, ArH); HRMS(ESI): Calcd for $C_{22}H_{16}BrFN_2O_4$ $[M+K]^+$ 508.9964. Found: 508.9915.

4.5.3. Data for 8c

White solid, yield, 44%, mp 100–101 °C. ^{1}H NMR(600 MHz, $CDCl_3$):δ 1.91 (s, 3H, Het–CH_3), 2.26 (s, 6H, Ar-2×CH3), 5.85 (s, 1H, NH), 6.94 (t, J = 7.5 Hz, 1H, ArH), 6.98–7.02 (m, 6H, ArH), 7.16 (t, J = 7.5 Hz, 1H, ArH), 7.37 (t, J = 8.1 Hz, 2H, ArH), 7.50 (d, J = 9.0 Hz, 2H, ArH); HRMS(ESI): Calcd for $C_{24}H_{22}N_2O_4$ $[M+K]^+$ 441.1259. Found: 441.1217.

4.5.4. Data for 8d

White solid, yield, 57%, mp 174–175 °C. ^{1}H NMR(600 MHz, $CDCl_3$): δ 1.99 (s, 3H, Het–CH_3), 6.03 (s, 1H, NH), 6.64 (d, J = 8.4 Hz, 2H, ArH), 7.04 (t, J = 4.2 Hz, 4H, ArH), 7.17 (s, 1H, ArH), 7.38 (dd, J = 8.4 and 15.0 Hz, 4H, ArH), 7.52 (d, J = 9.0 Hz, 2H, ArH); HRMS(ESI): Calcd for $C_{22}H_{17}BrN_2O_4$ $[M+H]^+$ 453.1701. Found: 453.0450.

4.5.5. Data for 8e

White solid, yield, 47%, mp 166–167 °C. ^{1}H NMR(400 MHz, $CDCl_3$): δ 2.01 (s, 3H, Het–CH_3), 6.25 (s, 1H, NH), 6.76 (d, J = 8.4 Hz, 2H, ArH), 7.04–7.07 (m, 4H, ArH), 7.18 (t, J = 7.2 Hz, 1H, ArH), 7.39 (t, J = 8.0 Hz, 2H, ArH), 7.50–7.55 (m, 4H, ArH); HRMS(ESI): Calcd for $C_{23}H_{17}F_3N_2O_4$ $[M+Na]^+$ 465.1072. Found: 465.1038.

4.5.6. Data for 8f

Yellow oil, yield, 53%. ^{1}H NMR(600 MHz, $CDCl_3$): δ 2.05 (s, 3H, Het–CH_3), 6.34 (s, 1H, NH), 6.72 (d, J = 7.8 Hz, 2H, ArH), 7.05 (t, J = 7.8 Hz, 4H, ArH), 7.19 (d, J = 7.8 Hz, 1H, ArH), 7.39 (t, J = 8.1 Hz, 2H, ArH), 7.54 (t, J = 6.3 Hz, 4H, ArH); HRMS(MALDI): Calcd for $C_{23}H_{17}N_3O_4$ $[M+K]^+$ 438.0842. Found: 438.0856.

4.5.7. Data for 8g

White solid, yield, 41%, mp 158–159 °C. ^{1}H NMR(600 MHz, $CDCl_3$): δ 1.98 (s, 3H, Het–CH_3), 2.27 (s, 3H, Ar-CH_3), 5.97 (s, 1H, NH), 6.69 (d, J = 8.4 Hz, 2H, ArH), 7.05 (dd, J = 8.4 and 12.6 Hz, 6H, ArH), 7.17 (d, J = 7.2 Hz, 1H, ArH), 7.37 (t, J = 7.8 Hz, 2H, ArH), 7.53 (d, J = 9.0 Hz, 2H, ArH); HRMS(MALDI): Calcd for $C_{23}H_{20}N_2O_4$ $[M+Na]^+$ 411.1454. Found: 411.1321.

4.5.8. Data for 8h

White solid, yield, 43%, mp 149–150 °C. ^{1}H NMR(600 MHz, $CDCl_3$): δ 1.99 (s, 3H, Het–CH_3), 6.03 (s, 1H, NH), 6.69 (d, J = 8.4 Hz, 2H, ArH), 7.05 (t, J = 4.5 Hz, 4H, ArH), 7.17 (s, 1H, ArH), 7.22 (d, J = 8.4 Hz, 2H, ArH), 7.38 (t, J = 7.8 Hz, 2H, ArH), 7.52 (d, J = 9.0 Hz, 2H, ArH); HRMS(ESI): Calcd for $C_{22}H_{17}ClN_2O_4$ $[M+K]^+$ 447.0519. Found: 447.0514.

4.5.9. Data for 8i

White solid, yield, 45%, mp 157–158 °C. ^{1}H NMR(600 MHz, $CDCl_3$): δ 1.96 (s, 3H, Het–CH_3), 3.76 (s, 3H, Ar–OCH_3), 5.90 (s, 1H, NH), 6.82 (dd, J = 9.0 and 20.4 Hz, 4H, ArH), 7.03 (d, J = 8.4 Hz, 4H, ArH), 7.16 (t, J = 7.5 Hz, 1H, ArH), 7.37 (t, J = 8.1 Hz, 2H, ArH), 7.52(d, J = 8.4 Hz, 2H, ArH); HRMS(MALDI): Calcd for $C_{23}H_{20}N_2O_5$ $[M+Na]^+$ 427.1271. Found: 427.1270.

4.5.10. Data for 8j

White solid, yield, 37%, mp 174–175 °C. ^{1}H NMR(600 MHz, $CDCl_3$): δ 1.99 (s, 3H, Het–CH_3), 2.24 (s, 3H, Ar-CH_3), 2.30 (s, 3H, Ar-CH_3), 5.90 (s, 1H, NH), 6.43 (d, J = 8.4 Hz, 1H, ArH), 6.88 (s, J = 7.8 Hz, 1H, ArH), 6.95(s, 1H, ArH), 7.04 (t, J = 9.0 Hz, 4H, ArH), 7.17 (d, J = 7.2 Hz, 1H, ArH), 7.37 (t, J = 7.8 Hz, 2H, ArH), 7.54 (d, J = 8.4 Hz, 2H, ArH); HRMS(MALDI): Calcd for $C_{24}H_{22}N_2O_4$ $[M+Na]^+$ 425.1491. Found: 425.1477.

4.5.11. Data for 8k

White solid, yield, 35%, mp 220–221 °C. ^{1}H NMR(400 MHz, $CDCl_3$): δ 2.03(s, 3H, Het–CH_3), 6.42 (s, 1H, NH), 6.68 (d, J = 8.4 Hz, 2H, ArH), 7.06 (dd, J = 3.6 and 8.4 Hz, 4H, ArH), 7.18 (s, 1H, ArH), 7.38 (d, J = 7.6 Hz, 2H, ArH), 7.96 (d, J = 8.4 Hz, 2H, ArH); HRMS(ESI): Calcd for $C_{23}H_{18}N_2O_6$ $[M+K]^+$ 457.0806. Found: 457.0802.

4.6. Enzyme assays

The preparation of succinate–cytochrome *c* reductase (SCR, mixture of respiratory complex II and bc_1 complex) from porcine heart was essentially as reported.[31] The activity of SCR was measured by monitoring the increase of cytochrome *c* at 550 nm, by using the extinction coefficient of 18.5 mM^{-1} cm^{-1}. The succinate–ubiquinone reductase (complex II) activity was measured by monitoring the decrease of 2,6-dichlorophenolindophenol (DCIP) at 600 nm, by using the extinction coefficient of 21 mM^{-1} cm^{-1}. The reaction mixture may be scaled down to 1.8 mL with final concentrations of PBS (pH 7.4), 100 mM; EDTA, 0.3 mM; succinate, 20 mM; oxidized cytochrome *c*, 60 μM (or DCIP, 53 μM); and appropriate amounts of enzyme to start the reaction.[32]

The ubiquinol–cytochrome *c* reductase (bc_1 complex) activity in catalyzing the oxidation of DBH_2 by cytochrome *c* was assayed in 100 mM PBS (pH 7.4), 0.3 mM EDTA, 750 μM lauryl maltoside (*n*-dodecyl-β-D-maltoside), 20–120 μM DBH_2, 100 μM oxidized cytochrome *c*, and an appropriate amount of SCR.[17] The preparation of DBH_2 from DB was carried out according to the procedure described in previous publications,[33,34] and the concentration of DBH_2 was determined by measuring the absorbance difference between 288 and 320 nm using an extinction coefficient of 4.14 mM^{-1} cm^{-1} for the calculation.[35,36] The nonionic detergent lauryl maltoside was used to decrease the interfering nonenzymatic oxidative activity,[19,35–37] though it was expected to affect the K_m value of the bc_1 complex for DBH_2.[19] For each reaction, the nonenzymatic rate for cytochrome *c* reduction was followed for at least 100 s before enzyme was added to initiate the reaction.[17]

For the steady state studies, the reaction was carried out in the absence or presence of various concentrations of the inhibitor. To obtain the K_i values, all reactions were initiated by the addition of enzyme and monitored continuously by following the absorbance change at certain wavelengths on a Perkin–Elmer Lambda 45 spectrophotometer equipped with a magnetic stirrer at 23 °C.

4.7. Data analysis

The concentrations at 50% inhibition (absolute IC_{50} values) for experiments with SCR were obtained from a nonlinear regression of the activity data according to a four parameter logistic model. The absolute IC_{50} was calculated according to Eq. 1.

$$y = \min + \frac{\max - \min}{1 + 10^{\log IC_{50} - x}} \quad (1)$$

The inhibition type was determined by Lineweaver–Burk plots, and computer fitted to the appropriate equations like Eqs. 2 and 3. Sigma Plot software 9.0 was used to determine all kinetic constants.

$$v = \frac{V_{max}[S]}{\left(1 + \frac{[I]}{K_I}\right)K_m + [S]} \quad (2)$$

$$v = \frac{V_{max}[S]}{\left(1 + \frac{[I]}{K_I}\right)(K_m + [S])} \quad (3)$$

Acknowledgments

The research was supported in part by the National Basic Research Program of China (No. 2010CB126103) and the NSFC (Nos. 20925206, 20932005, and 20872045). The authors also acknowledge Dr. Z. X. Wang for critical discussions and reading of the manuscript.

References and notes

1. Kim, H.; Xia, D.; Yu, C. A.; Xia, J. Z.; Kachurin, A. M.; Zhang, L.; Yu, L.; Deisenhofer, J. *Proc. Natl. Acad. Sci. U.S.A.* **1998**, *95*, 8026.
2. Gao, X. G.; Wen, X. L.; Yu, G. A.; Esser, L.; Tsao, S.; Quinn, B.; Zhang, L.; Yu, L. D.; Xia, D. *Biochemistry* **2002**, *41*, 11692.
3. Berry, E. A.; Huang, L. S. *FEBS Lett.* **2003**, *555*, 13.
4. Esser, L.; Quinn, B.; Li, Y. F.; Zhang, M. Q.; Elberry, M.; Yu, L. D.; Yu, C. A.; Xia, D. *J. Mol. Biol.* **2004**, *341*, 281.
5. Sauter, H.; Steglich, W.; Anke, T. *Angew. Chem., Int. Ed.* **1999**, *38*, 1328.
6. Berry, E. A.; Huang, L. S. *Biochim. Biophys. Acta* **2011**. doi:10.1016/j.bbabio.2011.04.005.
7. Sternberg, J. A.; Geffken, D.; Adams, J. B., Jr.; Postages, R.; Sternberg, C. G.; Campbell, C. L.; Moberg, W. K. *Pest Manag. Sci.* **2001**, *57*, 143.
8. Meunier, B.; Fisher, N. *FEMS* **2008**, *8*, 183.
9. Wenz, T.; Covian, R.; Hellwig, P.; MacMillan, F.; Meunier, B.; Trumpower, B. L.; Hunte, C. *J. Biol. Chem.* **2007**, *282*, 3977.
10. Jordan, D. B.; Livingston, R. S.; Bisaha, J. J.; Duncan, K. E.; Pember, S. O.; Picollelli, M. A.; Schwartz, R. S.; Sternberg, J. A.; Tang, X. S. *Pest. Sci.* **1999**, *55*, 105.
11. Sierotzki, H.; Parisi, S.; Steinfeld, U.; Tenzer, I.; Poirey, S.; Gisi, U. *Pest Manag. Sci.* **2000**, *56*, 833.
12. Pasche, J. S.; Piche, L. M.; Gudmestad, N. C. *Plant Dis.* **2005**, *89*, 269.
13. Jordan, D. B.; Livingstone, R. S.; Bisaha, J. J.; Duncan, K. E.; Pember, S. O.; Picollelli, M. A.; Schwartz, R. S.; Sternberg, J. A.; Tang, X. S. *Pest. Sci.* **1999**, *55*, 197.
14. Huggett, M.J.; Whittingham, W.G.; Buchanan, K.I. PCT Int. Patent Appl. WO/1997/038995, 1997.
15. Gao, X. G.; Wen, X. L.; Yu, C. A.; Esser, L.; Tsao, S.; Quinn, B.; Zhang, L.; Yu, L.; Xia, D. *Biochemistry* **2002**, *41*, 11692.
16. Pember, S. O.; Fleck, L. C.; Moberg, W. K.; Walker, M. P. *Arch. Biochem. Biophys.* **2005**, *435*, 280.
17. Zhao, P. L.; Wang, L.; Zhu, X. L.; Huang, X. Q.; Zhan, C. G.; Wu, J. W.; Yang, G. F. *J. Am. Chem. Soc.* **2010**, *132*, 185.
18. Chen, J. F.; Chen, C. L.; Alevriadou, B. R.; Zweier, J. L.; Chen, Y. R. *Biochim. Biophys. Acta* **2011**. doi:10.1016/j.bbabio.2011.03.001.
19. Chretien, D.; Slama, A.; Brière, J.; Munnich, A.; Rotig, A.; Rustin, P. *Curr. Med. Chem.* **2004**, *11*, 233.
20. Telford, J. E.; Kilbride, S. M.; Davey, G. P. *J. Biol. Chem.* **2010**, *285*, 8639.
21. Yu, A.; Yu, L.; King, T. E. *J. Biol. Chem.* **1974**, *249*, 4905.
22. Yu, A.; Yu, L. *Biochim. Biophys. Acta* **1980**, *591*, 409.
23. Schagger, H.; Pfeiffer, K. *J. Biol. Chem.* **2001**, *276*, 37861.
24. Gwak, S. H.; Yu, L.; Yu, C. A. *Biochemistry* **1986**, *25*, 7675.
25. Trécourt, F.; Breton, G.; Bonnet, V.; Mongin, F.; Marsais, F.; Quéguiner, G. *Tetrahedron* **2000**, *56*, 1349.
26. Johnnie, L.; Leazer, J.; Raymond, C. *Org. Syn.* **2005**, *82*, 115.
27. Ghosh, S.; Pardo, S. N.; Salomon, R. G. *J. Org. Chem.* **1982**, *47*, 4692.
28. Geffken, D.; Rayner, D. R. U.S. Patent 4957933, 1990.
29. Geffken, D.; Rayner, D. R. U.S. Patent 5223523, 1993.
30. Sternberg, J. A.; Sun, K. M.; Toji, M.; Witterholt, V. G. U.S. Patent 5552554, 1996.
31. Yu, L.; Yu, C. A. *J. Biol. Chem.* **1982**, *257*, 2016.
32. King, T. E. *Methods Enzymol.* **1967**, *10*, 216.
33. Rieske, J. S. *Methods Enzymol.* **1967**, *10*, 239.
34. Luo, C.; Long, J.; Liu, J. *Clin. Chim. Acta* **2008**, *395*, 38.
35. Fisher, N.; Bourges, I.; Hill, P.; Brasseur, G.; Meunier, B. *Eur.J. Biochem.* **2004**, *271*, 1292.
36. Fisher, N.; Brown, A. C.; Sexton, G.; Cook, A.; Windass, J.; Meunier, B. *Eur. J. Biochem.* **2004**, *271*, 2264.
37. Fisher, N.; Meunier, B. *Pest Manag. Sci.* **2005**, *61*, 973.